INTERNATIONAL JOURNAL FOR NUMERICAL METHODS IN FLUIDS
Int. J. Numer. Meth. Fluids **30**: 425–440 (1999)

A SEMI-IMPLICIT FINITE DIFFERENCE METHOD FOR NON-HYDROSTATIC, FREE-SURFACE FLOWS

VINCENZO CASULLI*

Department of Civil and Environmental Engineering, University of Trento, 38050 Mesiano di Povo, Trento, Italy

SUMMARY

In this paper a semi-implicit finite difference model for non-hydrostatic, free-surface flows is analyzed and discussed. It is shown that the present algorithm is generally more accurate than recently developed models for quasi-hydrostatic flows. The governing equations are the free-surface Navier–Stokes equations defined on a general, irregular domain of arbitrary scale. The momentum equations, the incompressibility condition and the equation for the free-surface are integrated by a semi-implicit algorithm in such a fashion that the resulting numerical solution is mass conservative and unconditionally stable with respect to the gravity wave speed, wind stress, vertical viscosity and bottom friction. Copyright © 1999 John Wiley & Sons, Ltd.

KEY WORDS: Navier–Stokes; shallow water; free-surface; semi-implicit; non-hydrostatic; three-dimensional

1. INTRODUCTION

The incompressible Navier–Stokes equations are known as being a valid model for many free-surface flow problems. Yet several simplified models have been derived from the Navier–Stokes equations to simulate specific flow problems in a determinate scale. Thus, for example, the two-dimensional vertically averaged shallow water equations are commonly used to study the circulation in well-mixed shallow estuaries, coastal seas and lakes [1–7]. High resolution of three-dimensional environmental flows can be obtained by solving numerically the three-dimensional hydrostatic primitive equations [8–12]. Three-dimensional hydrostatic models, however, are known to be ill-posed when used with open boundaries [13,14]. Moreover, problems where the hydrostatic approximation is no longer valid include flows over rapidly varying slopes and short waves where the ratio of the vertical to horizontal scales of motion is not sufficiently small.

Since these models have been derived from the Navier–Stokes equations under different simplifying assumptions, it appears clear that an accurate and efficient algorithm that solves directly the free-surface Navier–Stokes equations would apply to flows at different scales. One of the most popular numerical methods that successfully simulates free-surface flows for the Navier–Stokes equations is the marker-and-cell (MAC) method developed by Harlow and Welch [15]. The MAC method has been improved in several ways (see [16,17]), but the CFL stability restriction, relating the time step to the spatial discretization and to the free-surface

* Correspondence to: Department of Civil and Environmental Engineering, University of Trento, 38050 Mesiano di Povo, Trento, Italy.

CCC 0271–2091/99/120425–16$17.50

Received January 1998
Revised May 1998

wave speed, inhibits this method from being applied to three-dimensional geophysical flows with a sufficiently fine grid to resolve the small scale non-hydrostatic component of the flow. Moreover, a direct numerical approach to determine the three-dimensional pressure field is much too expensive from the computational point of view.

Recently, the three-dimensional Navier–Stokes equations have been integrated by a semi-implicit, fractional step method, where the hydrostatic pressure component is determined first and the non-hydrostatic component of the pressure is computed in a subsequent step [18–21]. This method is relatively simple, numerically stable even at large Courant numbers, and is suitable for simulations of complex three-dimensional flows where a small deviation from hydrostatic pressure is allowed.

In the present paper, the above scheme is further improved by including a correction for the free-surface in such a fashion that the new free-surface elevation is implicitly coupled with the non-hydrostatic pressure and with the new velocity field. In so doing, the splitting error is reduced, the resulting algorithm is locally and globally mass conservative, and applies to a wider class of free-surface problems ranging from hydrostatic to fully non-hydrostatic.

For hydrostatic and nearly hydrostatic flows, the present algorithm remains computationally competitive with the corresponding hydrostatic model. This method is accurate but requires a significant additional computational effort when applied to fully non-hydrostatic flows. In these cases, however, any hydrostatic model will yield totally different, and hence non-physical, results.

2. GOVERNING EQUATIONS

The governing three-dimensional, primitive variable equations describing the free-surface flows are the Navier–Stokes equations. Such equations express the physical principle of conservation of mass and momentum. The momentum equations for an incompressible fluid have the following form

$$\frac{\partial u}{\partial t}+u\frac{\partial u}{\partial x}+v\frac{\partial u}{\partial y}+w\frac{\partial u}{\partial z}=-\frac{\partial p}{\partial x}+\nu\left(\frac{\partial^2 u}{\partial x^2}+\frac{\partial^2 u}{\partial y^2}+\frac{\partial^2 u}{\partial z^2}\right), \tag{1}$$

$$\frac{\partial v}{\partial t}+u\frac{\partial v}{\partial x}+v\frac{\partial v}{\partial y}+w\frac{\partial v}{\partial z}=-\frac{\partial p}{\partial y}+\nu\left(\frac{\partial^2 v}{\partial x^2}+\frac{\partial^2 v}{\partial y^2}+\frac{\partial^2 v}{\partial z^2}\right), \tag{2}$$

$$\frac{\partial w}{\partial t}+u\frac{\partial w}{\partial x}+v\frac{\partial w}{\partial y}+w\frac{\partial w}{\partial z}=-\frac{\partial p}{\partial z}+\nu\left(\frac{\partial^2 w}{\partial x^2}+\frac{\partial^2 w}{\partial y^2}+\frac{\partial^2 w}{\partial z^2}\right)-g, \tag{3}$$

where $u(x, y, z, t)$, $v(x, y, z, t)$ and $w(x, y, z, t)$ are the velocity components in the horizontal x-, y- and vertical z-direction; t is the time; $p(x, y, z, t)$ is the normalized pressure defined as the pressure divided by a constant reference density; g is the gravitational acceleration; and ν is the kinematic viscosity coefficient. A complete model for field scale application would include the Coriolis acceleration, the baroclinic terms to account for density variations and non-constant turbulent viscosity coefficients (see [14,20,21]). For the sake of simplicity these terms have been omitted in the present work.

The mass conservation is expressed by the following incompressibility condition

$$\frac{\partial u}{\partial x}+\frac{\partial v}{\partial y}+\frac{\partial w}{\partial z}=0. \tag{4}$$

Integrating the continuity equation (4) over the depth and using the kinematic condition at the free-surface [10] leads to the following free-surface equation

$$\frac{\partial \eta}{\partial t}+\frac{\partial}{\partial x}\left[\int_{-h}^{\eta} u\,\mathrm{d}z\right]+\frac{\partial}{\partial y}\left[\int_{-h}^{\eta} v\,\mathrm{d}z\right]=0, \tag{5}$$

where $h(x, y)$ is the water depth measured from the undisturbed water surface and $\eta(x, y, t)$ is the free-surface elevation.

The pressure $p(x, y, z, t)$ in Equations (1)–(3) can be decomposed into the sum of its hydrostatic and a non-hydrostatic component. The hydrostatic pressure component is determined from the vertical momentum equation (3) by neglecting the convective and the viscous acceleration terms. Thus,

$$p(x, y, z, t)=g[\eta(x, y, t)-z]+q(x, y, z, t), \tag{6}$$

where $q(x, y, z, t)$ denotes the non-hydrostatic, or hydrodynamic pressure component. Thus, the momentum equations (1)–(3) can also be written as

$$\frac{\partial u}{\partial t}+u\frac{\partial u}{\partial x}+v\frac{\partial u}{\partial y}+w\frac{\partial u}{\partial z}=-g\frac{\partial \eta}{\partial x}-\frac{\partial q}{\partial x}+\nu\left(\frac{\partial^2 u}{\partial x^2}+\frac{\partial^2 u}{\partial y^2}+\frac{\partial^2 u}{\partial z^2}\right), \tag{7}$$

$$\frac{\partial v}{\partial t}+u\frac{\partial v}{\partial x}+v\frac{\partial v}{\partial y}+w\frac{\partial v}{\partial z}=-g\frac{\partial \eta}{\partial y}-\frac{\partial q}{\partial y}+\nu\left(\frac{\partial^2 v}{\partial x^2}+\frac{\partial^2 v}{\partial y^2}+\frac{\partial^2 v}{\partial z^2}\right), \tag{8}$$

$$\frac{\partial w}{\partial t}+u\frac{\partial w}{\partial x}+v\frac{\partial w}{\partial y}+w\frac{\partial w}{\partial z}=-\frac{\partial q}{\partial z}+\nu\left(\frac{\partial^2 w}{\partial x^2}+\frac{\partial^2 w}{\partial y^2}+\frac{\partial^2 w}{\partial z^2}\right). \tag{9}$$

When the hydrostatic approximation is made, Equation (9) is neglected and $q(x, y, z, t)=0$ is assumed throughout. In this case, the non-hydrostatic component of the pressure is assumed not to have effect on the resulting flow.

The boundary conditions at the free-surface are approximated by prescribing the wind stresses as

$$\nu\frac{\partial u}{\partial z}=\gamma_T(u_a-u), \qquad \nu\frac{\partial v}{\partial z}=\gamma_T(v_a-v), \tag{10}$$

where γ_T is a non-negative wind stress coefficient and u_a and v_a are the wind velocity components in the x- and in the y-direction respectively. At the bed, the bottom friction is specified by

$$\nu\frac{\partial u}{\partial z}=\gamma_B u, \qquad \nu\frac{\partial v}{\partial z}=\gamma_B v, \tag{11}$$

where γ_B is a non-negative bottom friction coefficient. Typically, γ_B can be derived from a turbulent boundary layer assumption.

3. NUMERICAL APPROXIMATION

In order to obtain an efficient numerical method whose stability is independent from the free-surface wave speed, wind stress, bottom friction and vertical viscosity, a semi-implicit fractional step scheme is derived. In the first step, the implicit contribution of the non-hydrostatic pressure is neglected and the gradient of surface elevation in the horizontal momentum equations (7) and (8), and the velocity in the free-surface equation (5), are discretized by the θ method [12]. Moreover, for stability, the wind stress, the vertical viscosity and the bottom friction will be discretized implicitly. In the second fractional step the provisional velocity and surface elevation are corrected by including the non-hydrostatic pressure terms, which are

calculated in such a fashion that the resulting velocity field is locally and globally mass conservative.

The physical domain is subdivided into $N_x N_y N_z$ rectangular cells of length Δx, width Δy and height $\Delta z_k = z_{k+1/2} - z_{k-1/2}$ respectively, where $z_{k\pm 1/2}$ are given level surfaces. Each cell is numbered at its center with indices i, j and k. The discrete u velocity is then defined at half integer i and integers j, k; v is defined at integers i, k and half integer j; w is defined at integers i, j and half integer k; q is defined at integers i, j and k; η is defined at integers i, j. Finally, the water depth $h(x, y)$ is specified at the u and v horizontal grid points.

3.1. First step: hydrostatic pressure

The first step of calculations is performed by neglecting the implicit contribution of the non-hydrostatic pressure. The resulting velocity field and water surface elevation at the new time level are not yet final and will be denoted by $\tilde{u}$, $\tilde{v}$, $\tilde{w}$ and $\tilde{\eta}$ respectively. A semi-implicit discretization for the momentum equations (7)–(9) takes the following form

$$\begin{aligned}\tilde{u}^{n+1}_{i+1/2,j,k} = {} & Fu^n_{i+1/2,j,k} - (1-\theta)\frac{\Delta t}{\Delta x}\left[g(\eta^n_{i+1,j} - \eta^n_{i,j}) + q^n_{i+1,j,k} - q^n_{i,j,k}\right] \\ & - \theta g \frac{\Delta t}{\Delta x}(\tilde{\eta}^{n+1}_{i+1,j} - \tilde{\eta}^{n+1}_{i,j}) \\ & + \nu \Delta t \frac{\dfrac{\tilde{u}^{n+1}_{i+1/2,j,k+1} - \tilde{u}^{n+1}_{i+1/2,j,k}}{\Delta z^n_{i+1/2,j,k+1/2}} - \dfrac{\tilde{u}^{n+1}_{i+1/2,j,k} - \tilde{u}^{n+1}_{i+1/2,j,k-1}}{\Delta z^n_{i+1/2,j,k-1/2}}}{\Delta z^n_{i+1/2,j,k}},\end{aligned} \tag{12}$$

$$\begin{aligned}\tilde{v}^{n+1}_{i,j+1/2,k} = {} & Fv^n_{i,j+1/2,k} - (1-\theta)\frac{\Delta t}{\Delta y}\left[g(\eta^n_{i,j+1} - \eta^n_{i,j}) + q^n_{i,j+1,k} - q^n_{i,j,k}\right] \\ & - \theta g \frac{\Delta t}{\Delta x}(\tilde{\eta}^{n+1}_{i,j+1} - \tilde{\eta}^{n+1}_{i,j}) \\ & + \nu \Delta t \frac{\dfrac{\tilde{v}^{n+1}_{i,j+1/2,k+1} - \tilde{v}^{n+1}_{i,j+1/2,k}}{\Delta z^n_{i,j+1/2,k+1/2}} - \dfrac{\tilde{v}^{n+1}_{i,j+1/2,k} - \tilde{v}^{n+1}_{i,j+1/2,k-1}}{\Delta z^n_{i,j+1/2,k-1/2}}}{\Delta z^n_{i,j+1/2,k}},\end{aligned} \tag{13}$$

$$\begin{aligned}\tilde{w}^{n+1}_{i,j,k+1/2} = {} & Fw^n_{i,j,k+1/2} - (1-\theta)\frac{\Delta t}{\Delta z^n_{i,j,k+1/2}}(q^n_{i,j,k+1} - q^n_{i,j,k}) \\ & + \nu \Delta t \frac{\dfrac{\tilde{w}^{n+1}_{i,j,k+3/2} - \tilde{w}^{n+1}_{i,j,k+1/2}}{\Delta z^n_{i,j,k+1}} - \dfrac{\tilde{w}^{n+1}_{i,j,k+1/2} - \tilde{w}^{n+1}_{i,j,k-1/2}}{\Delta z^n_{i,j,k}}}{\Delta z^n_{i,j,k+1/2}},\end{aligned} \tag{14}$$

where the vertical space increment Δz is usually defined as the distance between two consecutive level surfaces, except near the bottom and near the free-surface, where Δz is the distance between a level surface and bottom or free-surface respectively. Thus, in general, Δz depends on the spatial location, and near the free-surface it also depends on the time step. The vertical space increment Δz is also allowed to vanish in order to account for variable geometries and for the wetting and drying of tidal flats. Of course, the corresponding momentum equation (12), (13) or (14) is not defined at a grid point characterized by $\Delta z = 0$.

In Equations (12)–(14), F is a finite difference operator that includes the explicit discretization of the convective and horizontal viscosity terms. A particular form for F can be given in several ways, thus for example, by using an Eulerian–Lagrangian scheme (see, [10]). Equations

(12)–(14) also include appropriate discretizations of the boundary conditions (10) and (11) at the free-surface and at the bottom. For stability, the implicitness factor θ has to be chosen in the range $\frac{1}{2} \le \theta \le 1$ (for details see [12]).

For each i, j, the set of equations (14) forms a linear, tridiagonal system with unknowns $\tilde{w}^{n+1}_{i,j,k+1/2}$ on the same water column. The coefficient matrix of these systems is symmetric and positive definite. Thus, the provisional vertical component of the velocity can be readily determined by a direct method. Equations (12) and (13) also constitute a set of linear tridiagonal systems, that are however, coupled to the unknown water surface elevation $\tilde{\eta}^{n+1}$. In order to determine $\tilde{\eta}^{n+1}_{i,j}$, and for numerical stability, the provisional velocity field is required to satisfy, for each i, j, the discrete analogue of the free-surface equation (5),

$$\begin{aligned}
\tilde{\eta}^{n+1}_{i,j} = \eta^n_{i,j} &- \theta \frac{\Delta t}{\Delta x}\left[\sum_{k=m}^{M} \Delta z^n_{i+1/2,j,k}\tilde{u}^{n+1}_{i+1/2,j,k} - \sum_{k=m}^{M} \Delta z^n_{i-1/2,j,k}\tilde{u}^{n+1}_{i-1/2,j,k}\right] \\
&- \theta \frac{\Delta t}{\Delta y}\left[\sum_{k=m}^{M} \Delta z^n_{i,j+1/2,k}\tilde{v}^{n+1}_{i,j+1/2,k} - \sum_{k=m}^{M} \Delta z^n_{i,j-1/2,k}\tilde{v}^{n+1}_{i,j-1/2,k}\right] \\
&- (1-\theta)\frac{\Delta t}{\Delta x}\left[\sum_{k=m}^{M} \Delta z^n_{i+1/2,j,k}u^n_{i+1/2,j,k} - \sum_{k=m}^{M} \Delta z^n_{i-1/2,j,k}u^n_{i-1/2,j,k}\right] \\
&- (1-\theta)\frac{\Delta t}{\Delta y}\left[\sum_{k=m}^{M} \Delta z^n_{i,j+1/2,k}v^n_{i,j+1/2,k} - \sum_{k=m}^{M} \Delta z^n_{i,j-1/2,k}v^n_{i,j-1/2,k}\right],
\end{aligned} \tag{15}$$

where m and M, $1 \le m \le M \le N_z$, denote the lower and upper limit for the k-index representing the bottom and the top finite difference stencil respectively. Strictly speaking, m and M depend on their spatial location and M may also change with the time level to account for the free-surface dynamics. For notational simplicity, however, subscripts and superscript to m and M shall be omitted.

Upon multiplication by $\Delta z^n_{i+1/2,j,k}$ and $\Delta z^n_{i,j+1/2,k}$, Equations (12) and (13) are written in matrix notation as

$$\mathbf{A}^n_{i+1/2,j}\tilde{\mathbf{U}}^{n+1}_{i+1/2,j} = \mathbf{G}^n_{i+1/2,j} - \theta g \frac{\Delta t}{\Delta x}(\tilde{\eta}^{n+1}_{i+1,j} - \tilde{\eta}^{n+1}_{i,j})\mathbf{\Delta Z}^n_{i+1/2,j}, \tag{16}$$

$$\mathbf{A}^n_{i,j+1/2}\tilde{\mathbf{V}}^{n+1}_{i,j+1/2} = \mathbf{G}^n_{i,j+1/2} - \theta g \frac{\Delta t}{\Delta y}(\tilde{\eta}^{n+1}_{i,j+1} - \tilde{\eta}^{n+1}_{i,j})\mathbf{\Delta Z}^n_{i,j+1/2}, \tag{17}$$

where $\tilde{\mathbf{U}}$, $\tilde{\mathbf{V}}$, $\mathbf{\Delta Z}$, $\mathbf{G}$ and $\mathbf{A}$ are defined as follows:

$$\tilde{\mathbf{U}}^{n+1}_{i+1/2,j} = \begin{pmatrix} \tilde{u}^{n+1}_{i+1/2,j,M} \\ \tilde{u}^{n+1}_{i+1/2,j,M-1} \\ \vdots \\ \tilde{u}^{n+1}_{i+1/2,j,m} \end{pmatrix}, \qquad \tilde{\mathbf{V}}^{n+1}_{i,j+1/2} = \begin{pmatrix} \tilde{v}^{n+1}_{i,j+1/2,M} \\ \tilde{v}^{n+1}_{i,j+1/2,M-1} \\ \vdots \\ \tilde{v}^{n+1}_{i,j+1/2,m} \end{pmatrix}, \qquad \mathbf{\Delta Z} = \begin{pmatrix} \Delta z_M \\ \Delta z_{M-1} \\ \vdots \\ \Delta z_M \end{pmatrix},$$

$$\mathbf{G}^n_{i+1/2,j} = \begin{pmatrix} \Delta z_M\left\{Fu^n_{i+1/2,j,M} - (1-\theta)\dfrac{\Delta t}{\Delta x}[g(\eta^n_{i+1,j} - \eta^n_{i,j}) + q^n_{i+1,j,M} - q^n_{i,j,M}]\right\} + \gamma_T \Delta t u^{n+1}_a \\ \Delta z_{M-1}\left\{Fu^n_{i+1/2,j,M-1} - (1-\theta)\dfrac{\Delta t}{\Delta x}[g(\eta^n_{i+1,j} - \eta^n_{i,j}) + q^n_{i+1,j,M-1} - q^n_{i,j,M-1}]\right\} \\ \vdots \\ \Delta z_m\left\{Fu^n_{i+1/2,j,m} - (1-\theta)\dfrac{\Delta t}{\Delta x}[g(\eta^n_{i+1,j} - \eta^n_{i,j}) + q^n_{i+1,j,m} - q^n_{i,j,m}]\right\} \end{pmatrix},$$

$$\mathbf{G}^n_{i+1/2,j}=\begin{pmatrix}\Delta z_M\left\{Fv^n_{i,j+1/2,M}-(1-\theta)\dfrac{\Delta t}{\Delta y}\left[g(\eta^n_{i,j+1}-\eta^n_{i,j})+q^n_{i,j+1,M}-q^n_{i,j,M}\right]\right\}+\gamma_T\Delta t v_a^{n+1}\\ \Delta z_{M-1}\left\{Fv^n_{i,j+1/2,M-1}-(1-\theta)\dfrac{\Delta t}{\Delta y}\left[g(\eta^n_{i,j+1}-\eta^n_{i,j})+q^n_{i,j+1,M-1}-q^n_{i,j,M-1}\right]\right\}\\ \vdots\\ \Delta z_m\left\{Fu^n_{i,j+1/2,m}-(1-\theta)\dfrac{\Delta t}{\Delta y}\left[g(\eta^n_{i,j+1}-\eta^n_{i,j})+q^n_{i,j+1,m}-q^n_{i,j,m}\right]\right\}\end{pmatrix},$$

$$\mathbf{A}=\begin{pmatrix}\Delta z_M+a_{M-1/2}+\gamma_T\Delta t & -a_{M-1/2} & & 0\\ -a_{M-1/2} & \Delta z_{M-1}+a_{M-1/2}+a_{M-3/2} & -a_{M-3/2} & \\ \cdot & \cdot & \cdot & \\ & \cdot & \cdot & \cdot\\ 0 & & -a_{m+1/2} & \Delta z_m+a_{m+1/2}+\gamma_B\Delta t\end{pmatrix},$$

with $a_k=v\Delta t/\Delta z_k$.

Equation (15) can also be written using vector notation as

$$\tilde\eta^{n+1}_{i,j}=\delta^n_{i,j}-\theta\frac{\Delta t}{\Delta x}\left[(\mathbf{\Delta Z}^n_{i+1/2,j})^T\tilde{\mathbf{U}}^{n+1}_{i+1/2,j}-(\mathbf{\Delta Z}^n_{i-1/2,j})^T\tilde{\mathbf{U}}^{n+1}_{i-1/2,j}\right]$$
$$-\theta\frac{\Delta t}{\Delta y}\left[(\mathbf{\Delta Z}^n_{i,j+1/2})^T\tilde{\mathbf{V}}^{n+1}_{i,j+1/2}-(\mathbf{\Delta Z}^n_{i,j-1/2})^T\tilde{\mathbf{V}}^{n+1}_{i,j-1/2}\right],\tag{18}$$

where

$$\delta^n_{i,j}=\eta^n_{i,j}-(1-\theta)\frac{\Delta t}{\Delta x}\left[(\mathbf{\Delta Z}^n_{i+1/2,j})^T\mathbf{U}^n_{i+1/2,j}-(\mathbf{\Delta Z}^n_{i-1/2,j})^T\mathbf{U}^n_{i-1/2,j}\right]$$
$$-(1-\theta)\frac{\Delta t}{\Delta y}\left[(\mathbf{\Delta Z}^n_{i,j+1/2})^T\mathbf{V}^n_{i,j+1/2}-(\mathbf{\Delta Z}^n_{i,j-1/2})^T\mathbf{V}^n_{i,j-1/2}\right].$$

Formal substitution of the expressions for $\tilde{\mathbf{U}}^{n+1}_{i\pm1/2,j}$ and $\tilde{\mathbf{V}}^{n+1}_{i,j\pm1/2}$ from (16) and (17) into (18) yields

$$\tilde\eta^{n+1}_{i,j}-g\theta^2\frac{\Delta t^2}{\Delta x^2}\left\{[(\mathbf{\Delta Z})^T\mathbf{A}^{-1}\mathbf{\Delta Z}]^n_{i+1/2,j}(\tilde\eta^{n+1}_{i+1,j}-\tilde\eta^{n+1}_{i,j})\right.$$
$$\left.-[(\mathbf{\Delta Z})^T\mathbf{A}^{-1}\mathbf{\Delta Z}]^n_{i-1/2,j}(\tilde\eta^{n+1}_{i,j}-\tilde\eta^{n+1}_{i-1,j})\right\}$$
$$-g\theta^2\frac{\Delta t^2}{\Delta y^2}\left\{[(\mathbf{\Delta Z})^T\mathbf{A}^{-1}\mathbf{\Delta Z}]^n_{i,j+1/2}(\tilde\eta^{n+1}_{i,j+1}-\tilde\eta^{n+1}_{i,j})-[(\mathbf{\Delta Z})^T\mathbf{A}^{-1}\mathbf{\Delta Z}]^n_{i,j-1/2}(\tilde\eta^{n+1}_{i,j}-\tilde\eta^{n+1}_{i,j-1})\right\}$$
$$=\delta^n_{i,j}-\theta\frac{\Delta t}{\Delta x}\left\{[(\mathbf{\Delta Z})^T\mathbf{A}^{-1}\mathbf{G}]^n_{i+1/2,j}-[(\mathbf{\Delta Z})^T\mathbf{A}^{-1}\mathbf{G}]^n_{i-1/2,j}\right\}$$
$$-\theta\frac{\Delta t}{\Delta y}\left\{[(\mathbf{\Delta Z})^T\mathbf{A}^{-1}\mathbf{G}]^n_{i,j+1/2}-[(\mathbf{\Delta Z})^T\mathbf{A}^{-1}\mathbf{G}]^n_{i,j-1/2}\right\}.\tag{19}$$

Since the matrix $\mathbf{A}$ is an M-matrix, $\mathbf{A}^{-1}$ has non-negative elements everywhere. Therefore, the quantity $(\mathbf{\Delta Z})^T\mathbf{A}^{-1}\mathbf{\Delta Z}$ is itself non-negative everywhere. Hence, Equation (19) constitutes

a five-diagonal system of equations for the unknowns $\tilde{\eta}_{i,j}^{n+1}$. This system is strictly diagonally dominant, symmetric and positive definite, thus its unique solution can be determined by preconditioned conjugate gradient iterations until the residual norm becomes smaller than a given tolerance ϵ_η. Once the new free-surface location has been computed, Equations (16) and (17) are used to determine $\tilde{\mathbf{U}}_{i+1/2,j}^{n+1}$ and $\tilde{\mathbf{V}}_{i,j+1/2}^{n+1}$ throughout the computational domain.

3.2. Second step: non-hydrostatic correction

In the second step of calculations, the new velocity field $u_{i+1/2,j,k}^{n+1}$, $v_{i,j+1/2,k}^{n+1}$, $w_{i,j,k+1/2}^{n+1}$ and the new water surface elevation $\eta_{i,j}^{n+1}$ are computed by correcting the provisional values after including the non-hydrostatic pressure terms. Specifically, the discrete momentum equations are taken to be

$$u_{i+1/2,j,k}^{n+1} = \tilde{u}_{i+1/2,j,k}^{n+1} - \theta \frac{\Delta t}{\Delta x}(q_{i+1,j,k}^{n+1} - q_{i,j,k}^{n+1}), \tag{20}$$

$$v_{i,j+1/2,k}^{n+1} = \tilde{v}_{i,j+1/2,k}^{n+1} - \theta \frac{\Delta t}{\Delta y}(q_{i,j+1,k}^{n+1} - q_{i,j,k}^{n+1}), \tag{21}$$

$$w_{i,j,k+1/2}^{n+1} = \tilde{w}_{i,j,k+1/2}^{n+1} - \theta \frac{\Delta t}{\Delta z_{i,j,k+1/2}^{n}}(q_{i,j,k+1}^{n+1} - q_{i,j,k}^{n+1}) \tag{22}$$

and, in each computational cell below the free-surface, the discretized incompressibility condition (4) in finite volume form is taken to be

$$\frac{u_{i+1/2,j,k}^{n+1}\Delta z_{i+1/2,j,k}^{n} - u_{i-1/2,j,k}^{n+1}\Delta z_{i-1/2,j,k}^{n}}{\Delta x} + \frac{v_{i,j+1/2,k}^{n+1}\Delta z_{i,j+1/2,k}^{n} - v_{i,j-1/2,k}^{n+1}\Delta z_{i,j-1/2,k}^{n}}{\Delta y}$$
$$+ w_{i,j,k+1/2}^{n+1} - w_{i,j,k-1/2}^{n+1} = 0, \quad k = m, m+1, \ldots, M-1. \tag{23}$$

At the free-surface, the difference approximation of Equation (5) is

$$\eta_{i,j}^{n+1} = \delta_{i,j}^{n} - \theta \frac{\Delta t}{\Delta x}\left[\sum_{k=m}^{M} \Delta z_{i+1/2,j,k}^{n} u_{i+1/2,j,k}^{n+1} - \sum_{k=m}^{M} \Delta z_{i-1/2,j,k}^{n} u_{i-1/2,j,k}^{n+1}\right]$$
$$- \theta \frac{\Delta t}{\Delta y}\left[\sum_{k=m}^{M} \Delta z_{i,j+1/2,k}^{n} v_{i,j+1/2,k}^{n+1} - \sum_{k=m}^{M} \Delta z_{i,j-1/2,k}^{n} v_{i,j-1/2,k}^{n+1}\right], \tag{24}$$

which, by using (23), can also be written as

$$\eta_{i,j}^{n+1} = \delta_{i,j}^{n} - \theta \frac{\Delta t}{\Delta x}[\Delta z_{i+1/2,j,M}^{n} u_{i+1/2,j,M}^{n+1} - \Delta z_{i-1/2,j,M}^{n} u_{i-1/2,j,M}^{n+1}]$$
$$- \theta \frac{\Delta t}{\Delta y}[\Delta z_{i,j+1/2,M}^{n} v_{i,j+1/2,M}^{n+1} - \Delta z_{i,j-1/2,M}^{n} v_{i,j-1/2,M}^{n+1}] + \theta \Delta t w_{i,j,M-1/2}^{n+1}. \tag{25}$$

By assuming that the pressure in the surface cells is hydrostatic, the pressure correction $q_{i,j,M}^{n+1}$ is obtained from $g(\eta - z) = g(\tilde{\eta} - z) + q$. Hence, Equation (25) becomes

$$\frac{q_{i,j,M}^{n+1}}{g\theta\Delta t} = \frac{\delta_{i,j}^{n} - \tilde{\eta}_{i,j}^{n+1}}{\theta \Delta t} - \frac{\Delta z_{i+1/2,j,M}^{n} u_{i+1/2,j,M}^{n+1} - \Delta z_{i-1/2,j,M}^{n} u_{i-1/2,j,M}^{n+1}}{\Delta x}$$
$$- \frac{\Delta z_{i,j+1/2,M}^{n} v_{i,j+1/2,M}^{n+1} - \Delta z_{i,j-1/2,M}^{n} v_{i,j-1/2,M}^{n+1}}{\Delta y} + w_{i,j,M-1/2}^{n+1}. \tag{26}$$

An equation for the non-hydrostatic pressure $q_{i,j,k}^{n+1}$ is derived by substituting the expressions for the new velocities from (20)–(22) into (23) and (26) respectively. The following finite difference equations are obtained

$$\theta\Delta t\left[\frac{(q_{i+1,j,k}^{n+1}-q_{i,j,k}^{n+1})\Delta z_{i+1/2,j,k}^{n}-(q_{i,j,k}^{n+1}-q_{i-1,j,k}^{n+1})\Delta z_{i-1/2,j,k}^{n}}{\Delta x^2}\right.$$
$$+\frac{(q_{i,j+1,k}^{n+1}-q_{i,j,k}^{n+1})\Delta z_{i,j+1/2,k}^{n}-(q_{i,j,k}^{n+1}-q_{i,j-1,k}^{n+1})\Delta z_{i,j-1/2,k}^{n}}{\Delta y^2}$$
$$\left.+\frac{(q_{i,j,k+1}^{n+1}-q_{i,j,k}^{n+1})}{\Delta z_{i,j,k+1/2}^{n}}-\frac{(q_{i,j,k}^{n+1}-q_{i,j,k-1}^{n+1})}{\Delta z_{i,j,k-1/2}^{n}}\right]$$
$$=\frac{\tilde{u}_{i+1/2,j,k}^{n+1}\Delta z_{i+1/2,j,k}^{n}-\tilde{u}_{i-1/2,j,k}^{n+1}\Delta z_{i-1/2,j,k}^{n}}{\Delta x}+\frac{\tilde{v}_{i,j+1/2,k}^{n+1}\Delta z_{i,j+1/2,k}^{n}-\tilde{v}_{i,j-1/2,k}^{n+1}\Delta z_{i,j-1/2,k}^{n}}{\Delta y}$$
$$+\tilde{w}_{i,j,k+1/2}^{n+1}-\tilde{w}_{i,j,k-1/2}^{n+1}=0,\quad k=m,m+1,\ldots,M-1 \tag{27}$$

and

$$\theta\Delta t\left[\frac{(q_{i+1,j,M}^{n+1}-q_{i,j,M}^{n+1})\Delta z_{i+1/2,j,M}^{n}-(q_{i,j,M}^{n+1}-q_{i-1,j,M}^{n+1})\Delta z_{i-1/2,j,M}^{n}}{\Delta x^2}\right.$$
$$+\frac{(q_{i,j+1,M}^{n+1}-q_{i,j,M}^{n+1})\Delta z_{i,j+1/2,M}^{n}-(q_{i,j,M}^{n+1}-q_{i,j-1,M}^{n+1})\Delta z_{i,j-1/2,M}^{n}}{\Delta y^2}$$
$$\left.-\frac{(q_{i,j,M}^{n+1}-q_{i,j,M-1}^{n+1})}{\Delta z_{i,j,M-1/2}^{n}}\right]-\frac{q_{i,j,M}^{n+1}}{g\theta\Delta t}$$
$$=\frac{\tilde{\eta}_{i,j}^{n+1}-\delta_{i,j}^{n}}{\theta\Delta t}+\frac{\tilde{u}_{i+1/2,j,M}^{n+1}\Delta z_{i+1/2,j,M}^{n}-\tilde{u}_{i-1/2,j,M}^{n+1}\Delta z_{i-1/2,j,M}^{n}}{\Delta x}$$
$$+\frac{\tilde{v}_{i,j+1/2,M}^{n+1}\Delta z_{i,j+1/2,M}^{n}-\tilde{v}_{i,j-1/2,M}^{n+1}\Delta z_{i,j-1/2,M}^{n}}{\Delta y}-\tilde{w}_{i,j,M-1/2}^{n+1}. \tag{28}$$

The set of equations (27)–(28) form a seven-diagonal linear system. This system is diagonally dominant, with a strict inequality corresponding to Equation (28), moreover it is symmetric and positive definite. Thus, it can be solved by preconditioned conjugate gradient iterations until the residual norm is smaller than a given tolerance ϵ_q.

At the solid impenetrable boundaries, the condition of zero normal flux is imposed through Equations (20)–(22), which translates to a Neumann-type of boundary conditions on Equations (27) and (28). At the open boundaries either the normal velocity or the non-hydrostatic pressure should be specified. Accordingly, this translates into the Neumann- or Diriclet-type of boundary condition for Equations (27) and (28).

Once the non-hydrostatic pressure is computed, the corresponding horizontal velocity field is readily determined from Equations (20) and (21), while the vertical component of the velocity can be obtained, equivalently, either from (22) or from the incompressibility condition (23) which, by setting $w_{i,j,m-1/2}^{n+1}=0$ gives

$$w_{i,j,k+1/2}^{n+1}=w_{i,j,k-1/2}^{n+1}-\frac{u_{i+1/2,j,k}^{n+1}\Delta z_{i+1/2,j,k}^{n}-u_{i-1/2,j,k}^{n+1}\Delta z_{i-1/2,j,k}^{n}}{\Delta x}$$
$$-\frac{v_{i,j+1/2,k}^{n+1}\Delta z_{i,j+1/2,k}^{n}-v_{i,j-1/2,k}^{n+1}\Delta z_{i,j-1/2,k}^{n}}{\Delta y},\quad k=m,m+1,\ldots,M-1. \tag{29}$$

This latter choice guarantees that the resulting velocity field is discrete divergence free for any value of the tolerance ϵ_q. This choice enables the above algorithm to perform hydrostatic calculations by choosing ϵ_q to be a sufficiently large value.

Finally, the new free-surface elevation is given by the hydrostatic relation

$$\eta_{i,j}^{n+1} = \tilde{\eta}_{i,j}^{n+1} + \frac{q_{i,j,M}^{n+1}}{g} \tag{30}$$

and the vertical increments Δz are updated in order to account for the new free surface location.

4. PROPERTIES OF THE METHOD

In the present scheme the local mass conservation is assured by the finite volume form (23) used to discretize the incompressibility condition (4). Also, global mass conservation is guaranteed by Equation (24), which is a conservative discretization of the free-surface equation (5).

From a purely algebraic point of view, the present formulation does not require the calculation of the provisional free-surface as determined in the first fractional step by the linear system of Equation (19). Indeed, by choosing a tolerance ϵ_η sufficiently large so that no iterations will be required by the conjugate gradient method to solve system (19), the complete pressure field, including the water surface elevation, will be entirely determined in the second computational step by system (27) and (28), even in the case of hydrostatic flow. For computational convenience, however, accurate calculation of the provisional free-surface from the system of Equation (19) provides a better starting point for the iterations required by the preconditioned conjugate gradient method that determines the non-hydrostatic pressure. This is particularly the case for hydrostatic and quasi-hydrostatic calculations.

It is interesting to point out that the hydrostatic solution (also obtained with the semi-implicit algorithm described in [12]) can be naturally computed from the above non-hydrostatic algorithm by setting $q_{i,j,k}^0 = 0$, and by choosing a tolerance ϵ_q sufficiently large so that no iterations will be required by the conjugate gradient method to solve system (27) and (28). In this way the resulting hydrodynamic pressure component $q_{i,j,k}^{n+1}$ remains identically zero at every time step and the hydrostatic velocity field results from (20), (21), (29) and (30) as a particular case.

Another interesting consideration arises from the fact that if only one vertical layer is specified, one has $1 = m = M = N_z$ and the vertical spacing Δz represents the total water depth. In this particular case, the discrete incompressibility condition (23) does not apply and Equation (28) forms a linear and homogeneous system. This implies that the resulting pressure correction is identically zero and, accordingly, the calculations of the second fractional step are not required. Moreover, one can easily verify that in this case, Equations (12), (13) and (19) are a consistent semi-implicit discretization of the two-dimensional, vertically integrated shallow water equations [5].

The above property of the present algorithm leads to a general purpose computer code that can be used for both two-dimensional vertically averaged problems as well as hydrostatic and non-hydrostatic three-dimensional problems. More importantly, when the three-dimensional model is applied to a typical coastal plain tidal embayment characterized by deep channels connected to large and flat shallow areas, a great saving in computing time and memory requirement is achieved because the deep channels are correctly represented in three dimensions while the flat shallow areas are represented only in two dimensions.

For $\frac{1}{2} \leq \theta \leq 1$, the implicit coupling of the water surface elevation to the new velocity field renders this method unconditionally stable with respect to the speed of propagation of surface waves [12]. Additionally, the time step is not limited by wind stress, vertical viscosity or bottom friction because of the implicit discretization used for these terms in the first fractional step. When an Eulerian–Lagrangian discretization is used for the convective terms [10], a mild limitation on the time step is imposed by the explicit discretization of the horizontal eddy viscosity terms and is given by

$$\Delta t \leq \frac{1}{2\nu\left(\frac{1}{\Delta x^2}+\frac{1}{\Delta y^2}\right)}. \tag{31}$$

This condition is not a severe limitation in field scale applications, where the horizontal discretization steps Δx and Δy, typically are chosen to be much larger than Δz. Such a consideration justifies the choice of an implicit discretization for the wind stress, vertical viscosity and bottom friction from which the tridiagonal matrix $\mathbf{A}$ results.

5. APPLICATIONS

This section shows the importance of the non-hydrostatic pressure in situations that are relevant in several applications. In general, one might argue that hydrostatic models are capable of predicting the vertical structure of mainly horizontal flow. However, if the vertical component of the velocity is also of some importance, then hydrostatic models will not be accurate.

5.1. Oscillating basin

The first example deals with non-breaking waves resulting for a relatively large ratio of total depth $H = h + \eta$ to the wave length λ. In such a case, the hydrostatic pressure assumption does not apply, and for sufficiently small wave amplitude, the wave celerity c is approximated by the following dispersion relation:

$$c = \sqrt{\frac{g\lambda}{2\pi}\tanh\left(\frac{2\pi H}{\lambda}\right)}. \tag{32}$$

A square basin of length $L = 10$ m and depth $h = 10$ m is discretized with 400 square cells of equal sides $\Delta x = \Delta z = 0.5$ m. Starting with zero initial velocity, the flow is driven by an initial free-surface of constant slope $\eta = 0.02x - 0.1$. By neglecting bottom friction, horizontal and vertical viscosity, the calculation is carried out with a time step $\Delta t = 0.1$ s. The expected solution consists of a standing wave of length $\lambda = 2L$ and frequency $f = c/\lambda$, where c is given by the above dispersion relation. Figure 1 shows the water surface elevation at $x = 10$ m obtained with the present non-hydrostatic model and with an early, quasi-hydrostatic version of the present model [21]. The results clearly indicate that the wave amplitude computed with the present algorithm is in much better agreement with the analytical result approximated by the dispersion relation (32).

5.2. Wave propagation over a bar

The second example is concerned with spatial evolution of steep waves propagating over a longshore bar. To this purpose, the author refers to the Scheldt flume experiment carried at

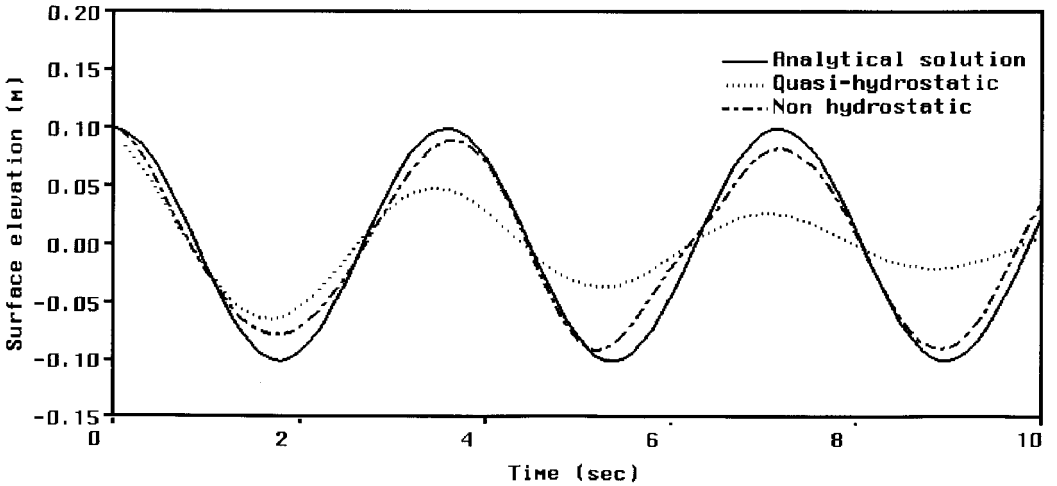

Figure 1. Free-surface wave of small amplitude.

Delft Hydraulics [22]. The flume has an overall length of 30 m. The bottom profile is shown in Figure 2. The still water depth was 0.4 m and reduced to 0.1 m over a submerged trapezoidal bar. At the end of the flume, a plane beach with a 1:25 slope serves as a wave absorber. The computational domain is discretized using $\Delta x = \Delta z_k = 2.5$ cm. A sinusoidal wave of amplitude 1 cm and period $T = 2.02$ s is specified at the left open boundary. The time step chosen for this simulation is $\Delta t = 0.025$ s. The resulting water surface elevation at three stations located at 13.5, 15.7 and 19 m from the open boundary is compared with the measurements in Figures 3–5 respectively. This example illustrates the potential of the present model in dealing with complex wave problems, even using a coarser mesh and larger time step than previous quasi-hydrostatic calculations [21]. For this example, the hydrostatic solution is totally different and of course, unrealistic.

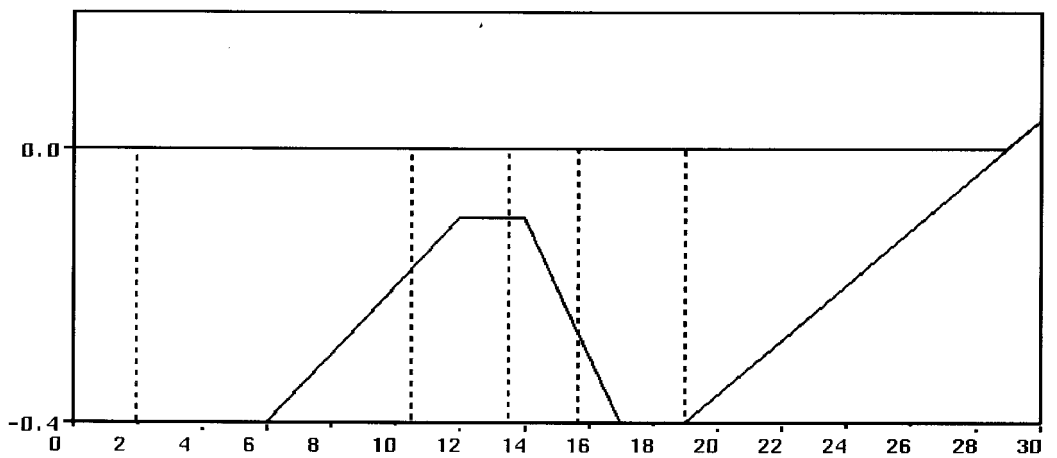

Figure 2. The wave flume geometry.

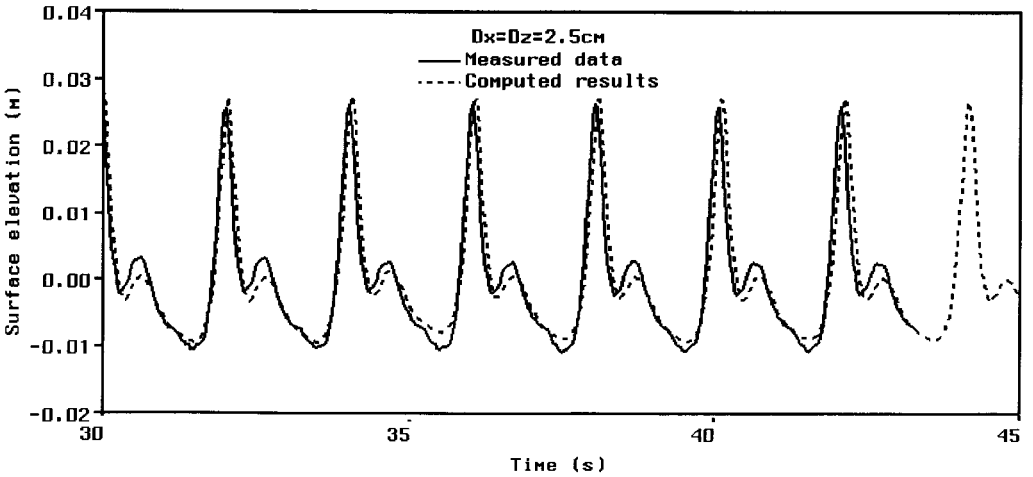

Figure 3. Water surface elevation at 13.5 m from the open boundary.

5.3. The Venice Lagoon

Finally, the present method has also been applied to simulate the three-dimensional flow in the Lagoon of Venice. The Lagoon of Venice covers an area of about 50 km^2 and consists of several inter-connected narrow channels with a maximum width of 1 km, and up to 50 m deep encircling large and flat shallow areas. The Lagoon is connected to the Adriatic Sea through three narrow inlets, namely Lido, Malamocco and Chioggia. A considerable portion of the Lagoon of Venice consists of tidal flats and proper treatment of flooding and drying is essential. Tidal waves propagate from the Adriatic Sea into the Lagoon through the three inlets. The Lagoon has been covered with a $672 \times 846 \times 200$ finite difference mesh of $\Delta x = \Delta y = 50$ m and with the maximum Δz being 0.25 m. Thus, the total number of grid points is 113 702 400, but only 1 637 508 of these are active. This fine computational mesh allows for a very accurate description of the tree-like structure of the main channels as shown in Figure

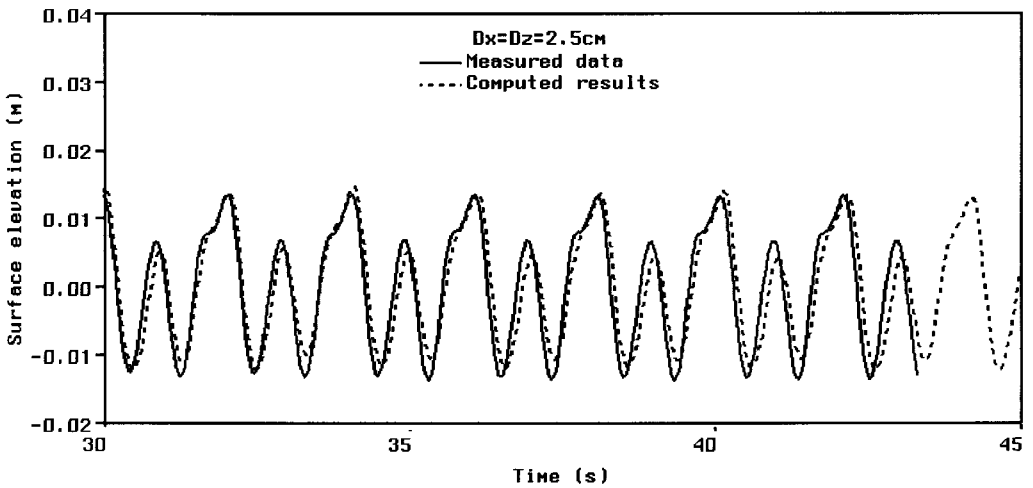

Figure 4. Water surface elevation at 15.7 m from the open boundary.

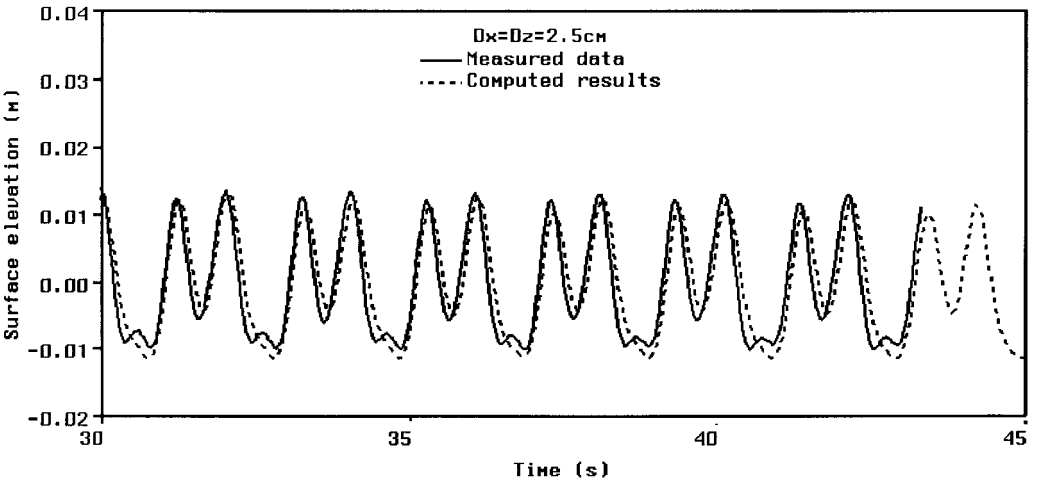

Figure 5. Water surface elevation at 19 m from the open boundary.

6. The fluid is driven at the three inlets, where an M_2 tide of 0.25 m amplitude and 12-h period has been specified. Figure 7 shows the maximum vertical speed obtained with and without the hydrostatic approximation and with a time step $\Delta t = 15$ min. This calculation was repeated with a time step $\Delta t = 0.15$ min and with a shorter driving wave of a 0.12-h period. Figure 8 shows a higher discrepancy between the hydrostatic and the non-hydrostatic results, thus indicating that, as expected, the hydrostatic approximation does not apply to medium and short waves.

6. CONCLUSIONS

A finite difference method for solving the three-dimensional Navier–Stokes equations has been outlined. The implicit coupling between the momentum and the free-surface equation renders this scheme unconditionally stable with respect to the surface wave speed. Moreover, since in geophysical flows the non-hydrostatic pressure is much smaller than the hydrostatic pressure, a significant improvement in computational efficiency has been achieved by decoupling the hydrostatic from the non-hydrostatic pressure. Thus, the hydrostatic pressure is determined by solving a five-diagonal linear system defined over the two-dimensional x–y domain, while to determine the non-hydrostatic pressure, fewer iterations on a larger seven-diagonal system are sufficient. The present algorithm is rather general, numerically stable and naturally reduces to a simpler hydrostatic model as a particular case. The computational examples given in this paper show that this algorithm is suitable for accurate simulation of geophysical flows as well as problems characterized by medium and short waves for which hydrostatic pressure alone is insufficient to obtain correct simulations. It can be concluded that this method enhances the range of problems that can be solved by computational methods for free-surface flows.

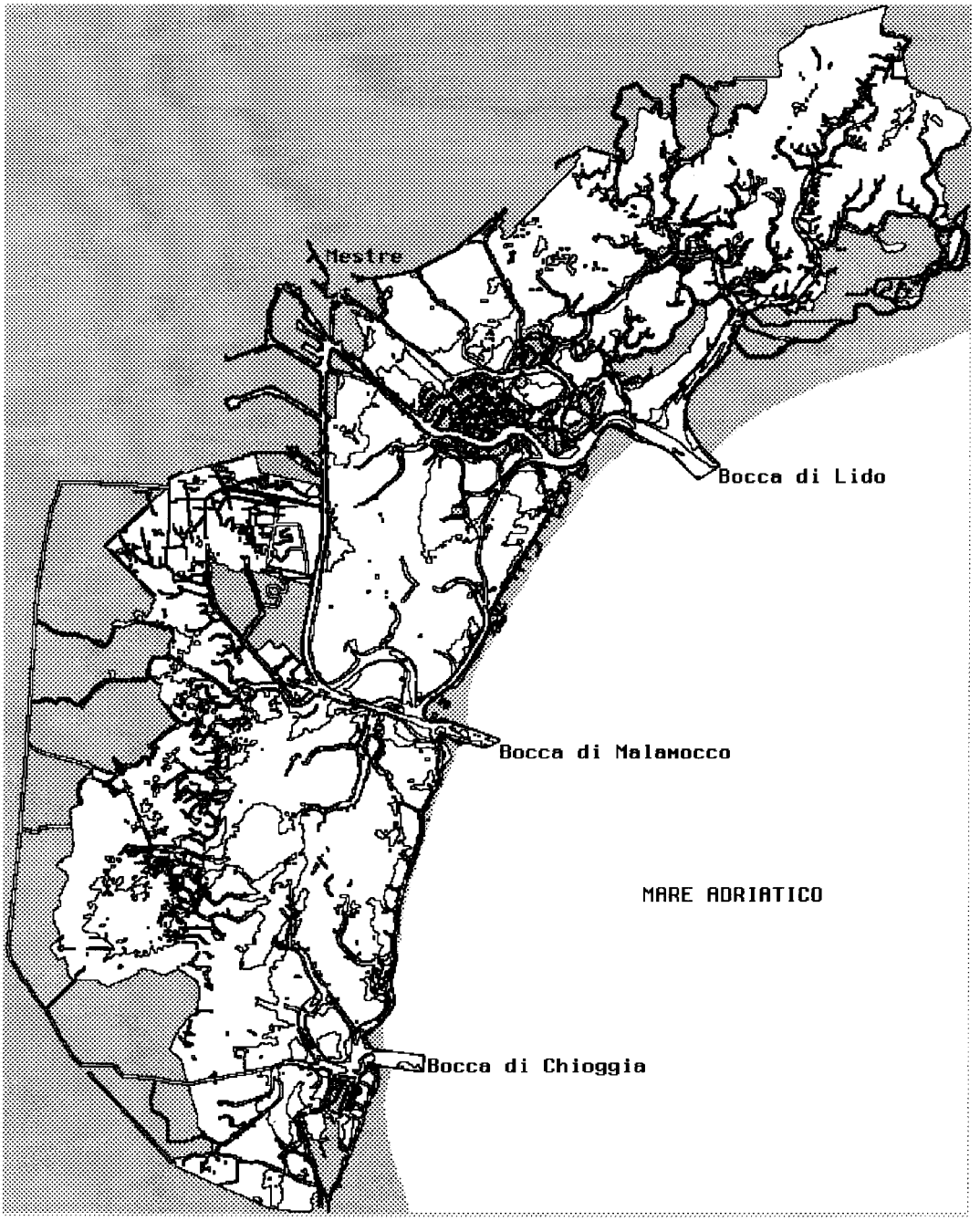

Figure 6. High resolution of the Venice Lagoon.

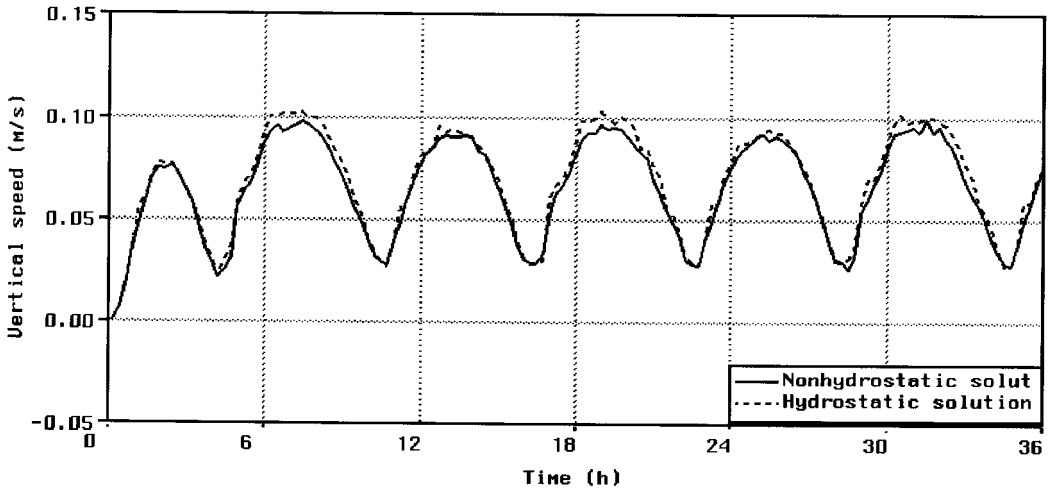

Figure 7. Maximum vertical speed in long waves.

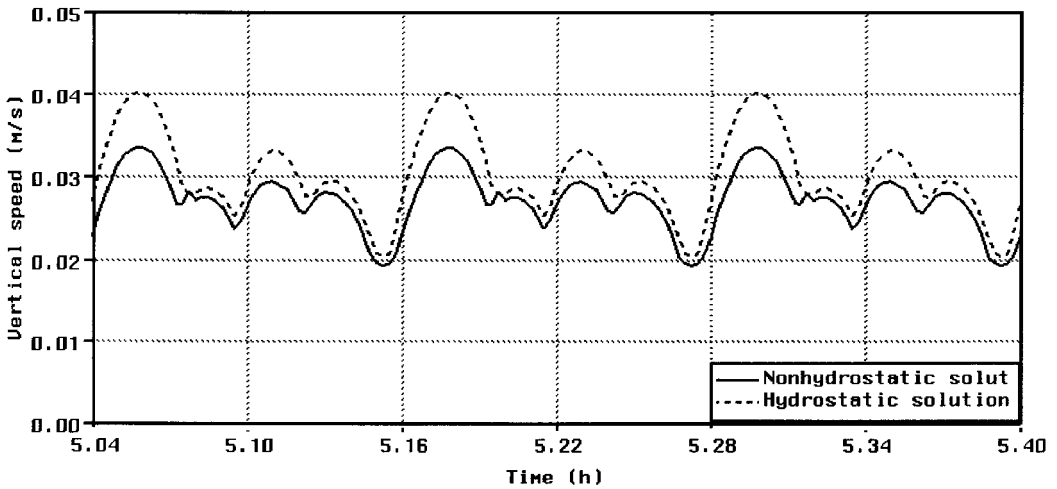

Figure 8. Maximum vertical speed in medium waves.

REFERENCES

1. J.J. Leendertse, 'Aspects of a computational method for long-period water wave propagation', *The RAND Corporation Memorandum RM-5294PR*, Santa Monica, CA, 1967.
2. J.P. Benqué, J.A. Cunge, J. Fuillet, A. Hauguel and F.M. Holly, 'New method of tidal current computation', *J. Waterway Port Ocean Div. ASCE*, **108**, 396–417 (1982).
3. G.S. Stelling, 'On the construction of computational methods for shallow water flow problems', *Rijkswaterstaat Communication No. 35*, The Hague, 1983.
4. P. Wilders, G.S. Stelling, L. van Th. Stijn and G.A. Fokkema, 'A fully implicit splitting method for accurate tidal computation', *Int. J. Numer. Methods Eng.*, **26**, 2707–2721 (1988).
5. V. Casulli, 'Semi-implicit finite difference methods for the two-dimensional shallow water equations', *J. Comput. Phys.*, **86**, 56–74 (1990).
6. R.P. Signell and B. Butman, 'Modeling tidal exchange and dispersion in Boston harbor', *J. Geophys. Res.*, **97**, 15591–15606 (1992).
7. R.T. Cheng, V. Casulli and J.W. Gartner, 'Tidal, residual, intertidal mudflat (TRIM) model and its applications to San Francisco Bay, California', *Estuar. Coast. Shelf Sci.*, **36**, 235–280 (1993).

8. A.F. Blumberg and G.L. Mellor, 'A description of a three-dimensional coastal ocean circulation model', in N.S. Heaps (ed.), *Three-Dimensional Coastal Ocean Circulation Models*, *Coastal and Estuarine Sciences*, vol. 4, AGU, Washington, DC, 1987, pp. 1–16.
9. J.J. Leendertse, 'A new approach to three-dimensional free-surface flow modelling', *The RAND Corporation Memorandum R-3712-NETH/RC*, Santa Monica, CA, 1989.
10. V. Casulli and R.T. Cheng, 'Semi-implicit finite difference methods for three-dimensional shallow water flow', *Int. J. Numer. Methods Fluids*, **15**, 629–648 (1992).
11. G.S. Stelling and J.J. Leendertse, 'Approximation of convective processes by cyclic AOI methods', in M.L. Spaulding, K. Bedford, A. Blumberg, R.T. Cheng and C. Swanson (eds.), *Proc. 2nd Int. Conf. on Estuarine and Coastal Modeling*, Tampa, FL, ASCE, 1992, pp. 771–782.
12. V. Casulli and E. Cattani, 'Stability, accuracy and efficiency of a semi-implicit method for three-dimensional shallow water flow', *Comput. Math. Appl.*, **27**, 99–112 (1994).
13. J. Oliger and A. Sundstrom, 'Theoretical and practical aspects of some initial boundary value problems in fluid dynamics', *SIAM J. Appl. Math.*, **35**, 419–446 (1978).
14. A. Mahadevan, J. Oliger and R. Street, 'A non-hydrostatic mesoscale ocean model. Part I: well posedness and scaling', *J. Phys. Oceanogr.*, **26**, 1868–1880 (1996).
15. F.H. Harlow and J.E. Welch, 'Numerical calculation of time dependent viscous, incompressible flow', *Phys. Fluids*, **8**, 2182–2189 (1965).
16. R.L. Street, R.K.C. Chan and J.E. Fromm, 'Two methods for the computation of the motion of long water waves—A review and applications', *8th Symp. on Naval Hydrodynamics: Hydrodynamics in the Ocean Environment*, *ARC-179*, Office of Naval Research, Washington DC, 1972, pp. 147–187.
17. M.F. Tome and S. McKee, 'GENSMAC: A computational marker and cell method for free-surface flows in general domains', *J. Comput. Phys.*, **110**, 171–186 (1994).
18. V. Casulli, 'Recent developments in semi-implicit numerical methods for free-surface hydrodynamics', *Advances in Hydro-Science and Engineering*, vol. 2, Tsinghua University Press, Beijing, 1995, pp. 2174–2181.
19. V. Casulli and G.S. Stelling, 'Simulation of three-dimensional, non-hydrostatic free-surface flows for estuaries and coastal seas', in M.L. Spaulding and R.T. Cheng (eds.), *Proc. 4th Int. Conf. on Estuarine and Coastal Modeling*, San Diego, CA, ASCE, 1996, pp. 1–12.
20. A. Mahadevan, J. Oliger and R. Street, 'A non-hydrostatic mesoscale ocean model. Part II: numerical implementation', *J. Phys. Oceanogr.*, **26**, 1881–1900 (1996).
21. V. Casulli and G.S. Stelling, 'Numerical simulation of three-dimensional quasi-hydrostatic, free-surface flows', *ASCE J. Hydraul. Eng.*, **124**, 678–686 (1998).
22. S. Beji and J.A. Battijes, 'Numerical simulation of non-linear waves propagation over a bar', *Coast. Eng.*, **23**, 1–16 (1994).

